Tailoring the Morphology of Carbon Nanotube Arrays: From Spinnable Forests to Undulating Foams

Yingying Zhang,[†,*] Guifu Zou,[†] Stephen K. Doorn,[†] Han Htoon,[†] Liliana Stan,[†] Marilyn E. Hawley,[†] Chris J. Sheehan,[†] Yuntian Zhu,[‡] and Quanxi Jia[†,*]

[†]Los Alamos National Laboratory, Los Alamos, New Mexico 87545, and [‡]Department of Material Science and Engineering, North Carolina State University, Raleigh, North Carolina 27695

ABSTRACT Directly spinning carbon nanotube (CNT) fibers from vertically aligned CNT arrays is a promising way for the application of CNTs in the field of high-performance materials. However, most of the reported CNT arrays are not spinnable. In this work, by controlling catalyst pretreatment conditions, we demonstrate that the degree of spinnability of CNTs is closely related to the morphology of CNT arrays. Shortest catalyst pretreatment time led to CNT arrays with the best spinnability, while prolonged pretreatment resulted in coarsening of catalyst particles and nonspinnable CNTs. By controlling the coalescence of catalyst particles, we further demonstrate the growth of undulating CNT arrays with uniform and tunable waviness. The CNT arrays can be tuned from well-aligned, spinnable forests to uniformly wavy, foam-like films. To the best of our knowledge, this is the first systematical study on the correlation between catalyst pretreatment, CNT morphology, and CNT spinnability.

KEYWORDS: carbon nanotube · CNT array · carbon nanotube fiber · catalyst pretreatment · spinnability · undulating structure

Since their discovery in 1991,[1] carbon nanotubes (CNTs) continue to be a subject of scientific research and development. The functionality of CNTs can be tailored by controlling their structures, geometries, and assembly.[2−8] Controlled growth of CNTs toward different functions remains a critical challenge for their applications in many fields. There is currently great interest in controlled synthesis of CNTs with unique structures.[9−18] CNT arrays, in which CNTs are nearly parallel to each other and perpendicular to the substrate, have been widely investigated for many potential applications, such as field emission devices,[3,18] energy storage,[13] gas sensors,[19] and structural composites.[20] Controlling the morphology of CNT arrays is an essential step toward these applications.

The extraordinary mechanical properties of CNTs promise CNT fiber to be a very promising candidate for next-generation ultrastrong and lightweight fibers.[5,6,21−26] They have been prepared by gas-state spinning from reaction furnace[21] and wet-spinning from CNT solutions,[22,23] in which case the performance of fibers is highly limited by CNT dispersion, alignment, and length. Much improved performance has been attained when continuous CNT ribbons were directly drawn from vertically aligned CNT arrays.[24] This process results in CNT fibers and CNT sheets with more interesting properties.[25,26] Following that, our group has achieved sustained growth of long (up to 1.5 mm) CNT arrays for fiber spinning and has produced CNT fibers with much improved strength and electrical conductivity.[5,6] It should be noted that many groups have successfully synthesized vertically aligned CNT arrays using Fe film as catalyst.[9,10,12,25−27] However, there exist only limited reports on the spinning of fibers from such CNT arrays.[5,25,26] This raises the question of why some CNT arrays are spinnable while others are not, given that the same catalyst and similar gas composition were used to produce the CNT arrays. It is well-known that catalysts (particle size and areal density) play an important role in determining the properties (CNT diameter and areal density) of CNT arrays.[12] On the other hand, bundle formation and alignment in CNT arrays are crucial for their spinnability.[26] Here, we report the key points to synthesis spinnable CNT arrays depending on the pretreatment of catalysts. We show that the shortest catalyst pretreatment leads to growth of CNT arrays with the best spinnability, while prolonged catalyst pretreatment results in disordered and nonspinnable CNTs. On the basis of understandings on the crucial role of catalyst pretreatment, we further demonstrate the growth of undulating CNT arrays with uniform and tunable waviness, which present a class of open-cell foam structures and may find a wide range of applications.

*Address correspondence to yyzhang@lanl.gov, qxjia@lanl.gov.

Received for review April 21, 2009 and accepted July 27, 2009.

Published online July 29, 2009.
10.1021/nn9003988 CCC: $40.75

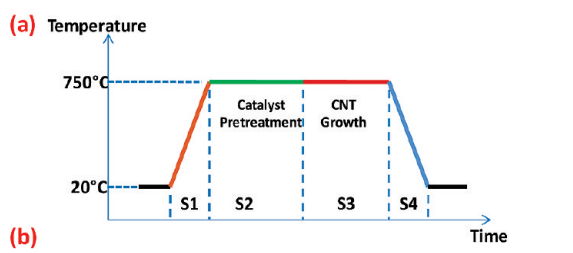

Samples	S1		S2		S3	
	Gas flow(sccm)	Time (min)	Gas flow(sccm)	Time (min)	Gas flow(sccm)	Time (min)
I-1	Forming gas (140) +C_2H_4 (30)	10	Forming gas (140)	0	Forming gas (140) +C_2H_4 (30)	10
I-2	Forming gas (140)	10	Forming gas (140)	0	Forming gas (140) +C_2H_4 (30)	10
I-3	Forming gas (140)	10	Forming gas (140)	10	Forming gas (140) +C_2H_4 (30)	10
I-4	Forming gas (140)	10	Forming gas (140)	60	Forming gas (140) +C_2H_4 (30)	10

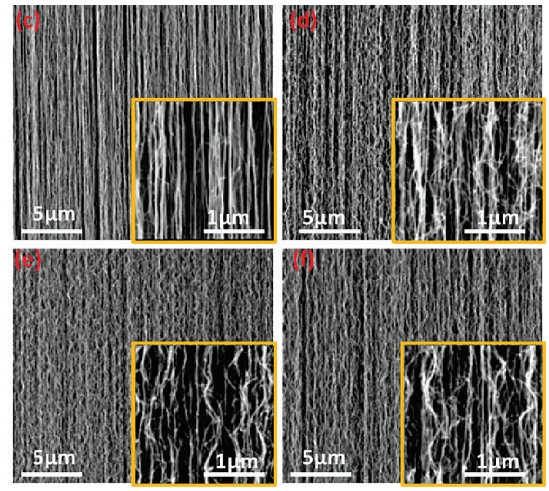

Figure 1. Effect of deposition process on the alignment of CNT array. (a) CVD process for CNT array growth, including four stages: S1, ramping up the temperature; S2, catalyst pretreatment; S3, CNT growth; S4, cooling down. (b) Gas composition and time for the first three stages of four samples. All of the samples are cooled in a flow of 140 sccm forming gas to room temperature (S4). (c−f) SEM images on the side view of four CNT arrays. The insets show magnified images. (c) Sample I-1, (d) sample I-2, (e) sample I-3, and (f) sample I-4.

Figure 1 shows our CVD process conditions and the resulting CNT arrays. A typical CVD process can be divided into four stages (Figure 1a): temperature ramping up (S1), catalyst pretreatment (S2), CNT growth (S3), and cooling down (S4). Using the same catalyst films, the CVD process for different samples is varied (Figure 1b). It should be noted that the carbon source was introduced at the beginning of S1 for sample I-1, which is quite different from the general CVD processes where the source gas should be introduced at the growth (S3) temperature. For the convenience of discussion, we define the catalyst pretreatment time for sample I-1 as −10 min (considering the introduction of C_2H_4 at S1), while that for samples I-2, I-3, and I-4 are 0, 10, and 60 min, respectively. Figure 1c−f shows clearly that prolonged catalyst pretreatment leads to increased disorder in CNT alignment. The CNTs of sample I-1 (Figure 1c) are straight and parallel to each other. In contrast, more curly CNTs are observed in sample I-2 (Figure 1d). This trend becomes much more obvious with longer catalyst pretreatment time. Most of the CNTs of sample I-4 are curly and show random orientations (Figure 1f).

The best spinnability was observed from the well-aligned CNT arrays (Figure 2a). With deteriorating vertical alignment, uneven ribbons containing big CNT blocks and broken CNT connections were observed (Figure 2b). In other words, long and uniform fibers up to meters can be easily prepared from sample I-1, while

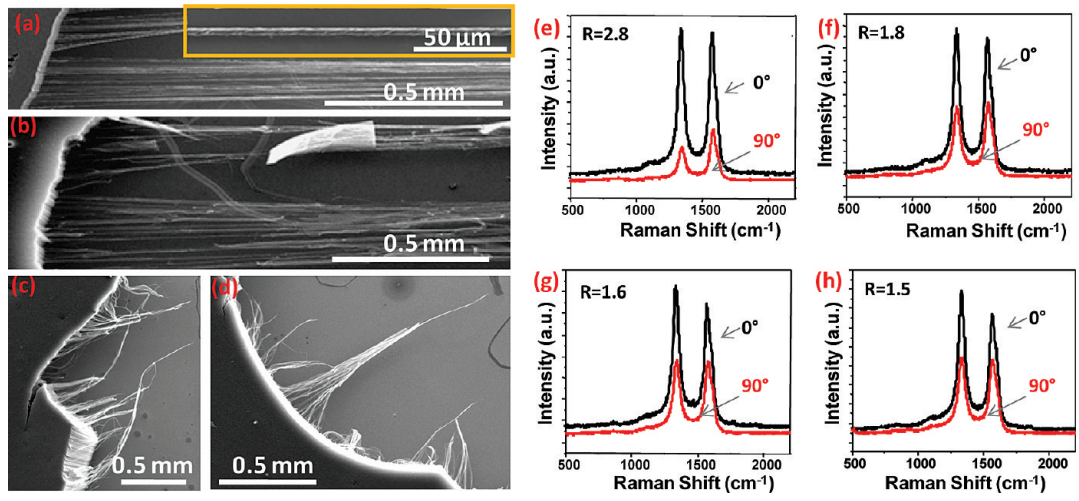

Figure 2. Effect of alignment on the spinnability of CNT array. (a−d) SEM images showing carbon nanotube ribbons pulled from sample I-1 (a), sample I-2 (b), sample I-3 (c), and sample I-4 (d), revealing the dependence of spinnability on the catalyst pretreatment time of CNT array. The inset of (a) shows SEM image of as-spun CNT fiber from sample I-1. (e−h) Polarized Raman spectra (532 nm) of the D and G bands from CNT array sample I-1 (e), sample I-2 (f), sample I-3 (g), and sample I-4 (h). The laser spot is focused on the side wall of CNT arrays; 0°, the polarization direction of the laser is parallel to the alignment of CNTs; 90°, the polarization direction of the laser is perpendicular to the alignment of CNTs. *R* is the intensity ratio of the G band between spectra obtained at 0 and 90° ($I_{G,0°}/I_{G,90°}$). The decreasing of *R* indicates that the alignment degree of CNTs is decreasing from sample I-1 to sample I-4.

only short fibers with lengths of centimeters may be spun from sample I-2. The spinnability drops dramatically with prolonged catalyst pretreatment. No continuous yarns can be drawn out from samples I-3 and I-4 (Figure 2c,d). These results suggest that the alignment of CNTs plays a critical role in the formation of continuous fibers. Good alignment of CNT arrays helps the formation of CNT bundles, which is a precondition for drawing out continuous CNT ribbons. Polarized Raman spectroscopy can give a quantitative measure of alignment of CNT arrays.[28] We find that the intensity ratio of the G band for polarizations parallel and perpendicular to the orientation of CNTs in the arrays decreases monotonically from sample I-1 to sample I-4 (Figure 2e−h). These results indicate that a much higher degree of alignment occurs in sample I-1. X-ray diffraction (XRD) has also been proven to be a useful tool to characterize the orientation of CNTs.[29] When the incident X-ray struck the top of arrays, the intensity of the (100) peak at 42.4° was observed to decrease dramatically from sample I-1 to I-4 (Supporting Information Figure S1).

It will be interesting to understand the limiting factors to grow highly aligned CNT arrays. Figure 3a illustrates our hypothesis on the evolution of catalyst particles and the morphological difference of the resulting CNT arrays. There are two main stages involved in the preparation of CNTs by CVD: the formation of catalyst particles and the nucleation/growth of CNTs from the catalyst. Under given processing conditions for the growth of CNTs, the formation of uniform and densely packed catalyst particles could be the key for growing well-aligned CNT arrays. The effect of H_2 pretreatment condition on the morphology of Fe/Al_2O_3 film has been reported.[30] Furthermore, the dependence of CNT diameter and areal density on the catalyst pretreatment has been very recently demonstrated.[12] In our process, the forming gas, containing 6% H_2 in Ar, works as a carrier gas as well as a reduction agent. It reduces the catalyst film and enables the formation of catalyst particles. At the same time, it will lead to the coarsening of catalyst particles. In the coarsening process, small catalyst particles tend to shrink and/or aggregate where their mass can be redistributed to larger particles. One can imagine the increase of the particle spacing due to the formation of large catalyst particles. This, in turn, will lead to the growth of CNTs with large diameters and low areal density. In our experiment, sample I-1 has the shortest catalyst pretreatment where the carbon source along with forming gas was introduced into the reaction chamber at the very beginning stage (S1). In this case, the nucleation of CNTs will occur as soon as the temperature is suitable. At the same time, the nucleation of CNTs will prevent the catalyst particles from growing larger. In contrast to sample I-1, the catalyst particles of other samples experienced a longer coarsening time, resulting in non-uniform and low area density of catalyst particles. These catalyst particles have the tendency to promote the growth of CNT arrays with poor alignment. Experimentally, the CNTs in sample I-1 should have smaller and more uniform diameters. They are more densely packed than in other samples, which helps the formation of CNT bundles and the much improved spinnability.

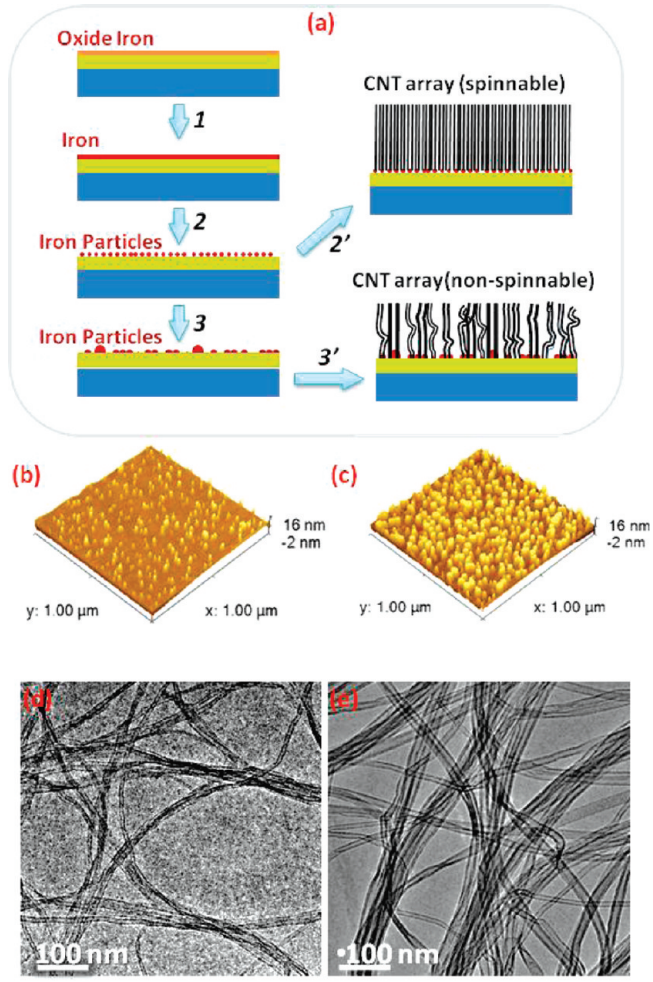

Figure 3. Evolution of catalyst film and the resulting CNT array. (a) Schematic illustration shows long catalyst pretreatment time leads to coarsening of catalyst particles, and the resulting CNT array is not uniform and not spinnable. 1: Reduction of iron oxide by H_2. 2: Formation of iron particles. 3: Coarsening of iron particles. 2′,3′: CNT growth by CVD. (b,c) AFM images of the catalyst film with pretreatment time of −10 and 60 min, respectively. (d,e) TEM images of CNTs derived from sample I-1 (catalyst pretreatment: −10 min) and sample I-4 (catalyst pretreatment: 60 min), respectively.

To validate the above hypothesis, atomic force microscopy (AFM) and transmission electron microscopy (TEM) were used to characterize the morphology of catalyst particles and the diameter of CNTs. Figure 3b,c shows AFM images of the catalyst films that have undergone −10 and 60 min pretreatments, corresponding to processing conditions of sample I-1 and sample I-4, respectively. Figure 3b shows a relatively smooth and uniform catalyst film with only scattered large catalyst particles, while Figure 3c is totally domi-

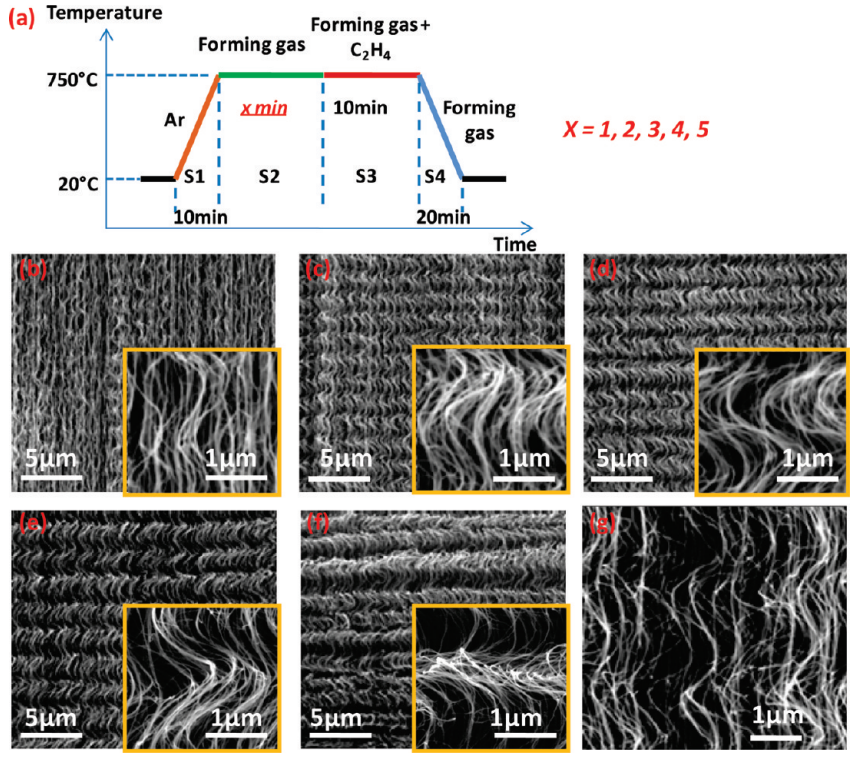

Figure 4. Growth of undulating CNT arrays. (a) CVD process for CNT array growth (sample II-1 to II-5) using Ar atmosphere for stage S1 and forming gas with varied time for pretreatment stage (S2). The gas atmosphere and time for each stage are marked in the illustration. (b−f) SEM images (side view) of CNT arrays synthesized according to the process shown in (a) with varied pretreatment time (duration of S2). (b) Sample II-1, 1 min; (c) sample II-2, 2 min; (d) sample II-3, 3 min; (e) sample II-4, 4 min; (f) sample II-5, 5 min. The insets show magnified images. (g) SEM image of sample II-2 showing the different curvatures of CNTs in the same array.

nated by large size catalyst particles. It is well-known that the size of catalyst particles has an important influence on the diameter of CNTs. Figure 3d,e shows the TEM images of CNTs derived from samples I-1 and I-4, respectively. The CNTs from sample I-1 have uniform diameters around 10 nm, while the diameters varied from 10 to 25 nm for sample I-4.

On the basis of the above understanding, we redesigned the process by replacing the forming gas (Ar/H_2) with pure Ar in step S1 (Figure 4a). Interestingly, we observed the growth of undulating CNTs. These undulating arrays were also characterized by Raman spectroscopy, which showed very similar Raman spectra, as shown in Figure 2, verifying that the obtained products are CNTs. Undulating CNT arrays, which are lightweight and super compressible, have been suggested to present a class of open-cell foam structures and may be useful as compliant interconnectors and energy dissipation coatings.[31] Considering the chemical activity of Fe at room temperature, the Fe catalyst film is assumed to be oxidized before starting the thermal process.[12] In the process shown in Figure 1a, the temperature ramping up stage (S1) is performed in forming gas, which allows the formation and coarsening of catalyst particles to occur in stage S1. In contrast, the use of pure Ar in the modified process (Figure 4a) prevents the reduction and dewetting of catalyst film until the introduction of H_2 (S2), thus helping to better control the catalyst pretreatment process. Using the process shown in Figure 4a, CNT growth was performed with catalyst pretreatment (S2) varied from 1 to 5 min (samples II-1 to II-5). The morphologies of the resulting CNTs show a very interesting undulating shape where the curvature increases with catalyst pretreatment time (Figure 4b−f). The intensity ratio of the Raman G band for polarizations parallel and perpendicular to the orientation of CNTs in the arrays shows a decreasing trend from sample II-1 ($R = 2.0$) to sample II-5 ($R = 1.1$), which is similar to the trend found in sample I-1 to sample I-4. These results are also consistent with the SEM images shown in Figure 4. The maximum in-plane displacements of CNTs also tend to keep increasing from samples II-1 to II-5 (Figure 4 and Supporting Information Figure S2). At the same time, the heights of arrays decreased rapidly with their increased curvature. The height of sample II-1 is 480 μm, while that of sample II-5 is only 100 μm. It should be noted that sample II-1 could be spun into short CNT fibers (several centimeters long) while others were not spinnable.

The mechanism for the formation of such uniform undulating CNT arrays is not fully understood yet. However, our experimental results do provide some insights. We argue that the size distribution of catalyst particles is responsible for this phenomenon. Similar to the situation shown in Figure 3a, long catalyst pretreatment will result in large catalyst particles. With both

small and large catalyst particles coexisting on the substrate, the growth rate of CNTs is not uniform. In other words, the growth rate of CNTs with smaller diameters is faster than that for larger diameters. Since the growth mode is base growth, the top of CNTs maintains the same distance from the substrate due to the van der Waals interactions between adjacent CNTs. Consequently, smaller diameter CNTs have to become wavy to match the height of larger diameter CNTs. This hypothesis is consistent with the magnified SEM image of sample II-2 (Figure 4g), where both straight and wavy CNTs can be clearly seen. Because long catalyst pretreatment leads to a broad size distribution of catalyst particles, prolonged pretreatment will lead to an aggravated difference in CNT growth rates. This, in return, results in large waviness in small diameter CNTs. It should be noted that the apparent height of arrays is mainly determined by the height of CNTs with large diameters. The trend of morphology change from sample II-1 to II-5 is consistent with this explanation.

In summary, we demonstrated that there is a close relationship between the catalyst pretreatment conditions and the spinnability of the resulting CNT arrays. The CNT arrays, grown by simultaneously introducing forming gas and ethylene in the CVD process, exhibit the best spinnability. In contrast, CNT arrays grown with prolonged catalyst pretreatment are disordered and not spinnable. The coarsening of catalyst particles during the pretreatment is believed to be the main reason for the formation of disordered CNTs. On the basis of these findings, a redesign of catalyst pretreatment process yields undulating foam-like CNTs.

METHODS

The CNT arrays were synthesized in a 2.54 cm diameter quartz tube furnace. A thin layer of Fe (~1.0 nm) catalyst film was deposited on Al_2O_3 (~10 nm) on SiO_2 (~1 μm) coated Si wafers. Forming gas (Ar with 6% H_2) was used as carrier gas, and ethylene served as carbon source. CNT growth was carried out at 750 °C for 10 min with 140 sccm forming gas and 30 sccm ethylene. Under such processing conditions, the effect of catalyst pretreatment on the morphology of CNT arrays was investigated by changing the time and gas environment of the catalyst pretreatment stage.

The spinnability of CNT arrays was investigated by using tweezers to pull out CNT yarns from the side walls of CNT arrays. A more controlled spin process can be performed by sticking the yarns on a spindle tip, which can move and spin at an adjustable speed. The CNT arrays and the CNT yarns pulled from different arrays were examined by scanning electron microscopy (SEM). Polarized Raman spectrocsopy (532.15 nm excitation) and X-ray diffraction (XRD) were used to examine the alignment of CNTs in arrays. Atomic force microscopy (AFM) was used to characterize the morphology of catalyst particles. The samples for AFM measurement were prepared by following the procedures shown in Figure 1a except for changing CNT growth time to 1 min (stage S3) and then burning off the CNTs at 600 °C for 30 min in air. Transmission electron microscopy (TEM) was used to characterize the diameters of CNTs. The samples for TEM measurement were prepared by drop CNTs/ethanol solutions onto copper grids in the open air.

Acknowledgment. We gratefully acknowledge the support of the U.S. Department of Energy (DOE) through the LANL/LDRD Program.

Supporting Information Available: XRD patterns of CNT arrays (Figure S1) and maximum in-plane displacement of CNTs of sample II-1 to II-5 (Figure S2). This material is available free of charge *via* the Internet at http://pubs.acs.org.

REFERENCES AND NOTES

1. Iijima, S. Helical Microtubules of Graphitic Carbon. *Nature* **1991**, *354*, 56–58.
2. Cao, Q.; Rogers, J. A. Random Networks and Aligned Arrays of Single-Walled Carbon Nanotubes for Electronic Device Applications. *Nano Res.* **2008**, *1*, 259–272.
3. Fan, S.; Chapline, M. G.; Franklin, N. R.; Tombler, T. W.; Cassell, A. M.; Dai, H. Self-Oriented Regular Arrays of Carbon Nanotubes and Their Field Emission Properties. *Science* **1999**, *283*, 512–514.
4. Cao, A.; Veedu, V. P.; Li, X.; Yao, Z.; Ghasemi-Nejhed, M. N.; Ajayan, P. M. Multifunctional Brushes Made from Carbon Nanotubes. *Nat. Mater.* **2005**, *4*, 540–545.
5. Li, Q.; Zhang, X.; Depaula, R. F.; Zheng, L.; Zhao, Y.; Stan, L.; Holesinger, T. G.; Arendt, P. N.; Peterson, D. E.; Zhu, Y. T. Sustained Growth of Ultralong Carbon Nanotube Arrays for Fiber Spinning. *Adv. Mater.* **2006**, *18*, 3160–3163.
6. Zhang, X.; Li, Q.; Holesinger, T. G.; Arendt, P. N.; Huang, J.; Kirven, P. D.; Clapp, T. G.; Depaula, R. F.; Liao, X.; Zhao, Y.; et al. Ultrastrong, Stiff, and Lightweight Carbon-Nanotube Fibers. *Adv. Mater.* **2007**, *19*, 4198–4201.
7. Sethi, S.; Ge, L.; Ci, L.; Ajayan, P. M.; Dhinojwala, A. Gecko-Inspired Carbon Nanotube-Based Self-Cleaning Adhensives. *Nano Lett.* **2008**, *8*, 822–825.
8. Engel, M.; Small, J. P.; Steiner, M.; Freitag, M.; Green, A. A.; Hersam, M. C.; Avouris, P. Thin Film Nanotube Transistors Based on Self-Assembled, Aligned, Semiconducting Carbon Nanotube Arrays. *ACS Nano* **2008**, *2*, 2445–2452.
9. Qu, L.; Du, F.; Dai, L. Preferential Syntheses of Semiconducting Vertically Aligned Single-Walled Carbon Nanotubes for Direct Use in FETs. *Nano Lett.* **2008**, *8*, 2682–2687.
10. Hart, A. J.; Slocum, A. H. Force Output, Control of Film Structure, and Microscale Shape Transfer by Carbon Nanotube Growth under Mechanical Pressure. *Nano Lett.* **2006**, *6*, 1254–1260.
11. Choi, K. M.; Augustine, A.; Choi, J. H.; Lee, J. H.; Yang, S. H.; Lee, J. Y.; Kang, J. K. A Facile Way to Control the Number of Walls in Carbon Nanotubes through the Synthesis of Exposed-Core/Shell Catalyst Nanoparticles. *Angew. Chem., Int. Ed.* **2008**, *47*, 9904–9907.
12. Nessim, G. D.; Hart, A. J.; Kim, J. S.; Acquaviva, D.; Oh, J.; Morgan, C. D.; Seita, M.; Leib, J. S.; Thompson, C. V. Tuning of Vertically-Aligned Carbon Nanotube Diameter and Areal Density through Catalyst Pre-Treatment. *Nano Lett.* **2008**, *8*, 3587–3593.
13. Talapatra, S.; Kar, S.; Pal, S. K.; Vajtai, R.; Ci, L.; Victor, P.; Shaijumon, M. M.; Kaur, S.; Nalamasu, O.; Ajayan, P. M. Direct Growth of Aligned Carbon Nanotubes on Bulk Metals. *Nat. Nanotechnol.* **2006**, *1*, 112–116.
14. Yao, Y.; Li, Q.; Zhang, J.; Liu, R.; Jiao, L.; Zhu, Y.; Liu, Z. Temperature-Mediated Growth of Single-Walled Carbon-Nanotube Intramolecular Junctions. *Nat. Mater.* **2007**, *6*, 283–286.
15. Geblinger, N.; Ismach, A.; Joselevich, E. Self-Organized Nanotube Serpentines. *Nat. Nanotechnol.* **2008**, *3*, 195–200.
16. Pint, C. L.; Xu, Y. Q.; Pasquali, M.; Hauge, R. H. Formation of Highly Dense Aligned Ribbons and Transparent Films of

Single-Walled Carbon Nanotubes Directly from Carpets. *ACS Nano* **2008**, *2*, 1871–1878.
17. Sumpter, B. G.; Meunier, V.; Romo-Herrera, J. M.; Cruz-Silva, E.; Cullen, D. A.; Terrones, H.; Smith, D. J.; Terrones, M. Nitrogen-Mediated Carbon Nanotube Growth: Diameter Reduction, Metallicity, Bundle Dispersability, and Bamboo-like Structure Formation. *ACS Nano* **2007**, *1*, 369–375.
18. Zhao, B.; Futaba, D. N.; Yasuda, S.; Akoshima, M.; Yamada, T.; Hata, K. Exploring Advantages of Diverse Carbon Nanotube Forests with Tailored Structures Synthesized by Supergrowth from Engineered Catalysts. *ACS Nano* **2009**, *3*, 108–114.
19. Wei, C.; Dai, L.; Roy, A.; Tolle, T. B. Multifunctional Chemical Vapor Sensors of Aligned Carbon Nanotube and Polymer Composites. *J. Am. Chem. Soc.* **2006**, *128*, 1412–1413.
20. Ci, L.; Suhr, J.; Pushparaj, V.; Zhang, X.; Ajayan, P. M. Continuous Carbon Nanotube Reinforced Composites. *Nano Lett.* **2008**, *8*, 2762–2766.
21. Li, Y. L.; Kinloch, I. A.; Windle, A. H. Direct Spinning of Carbon Nanotube Fibers from Chemical Vapor Deposition Synthesis. *Science* **2004**, *304*, 276–278.
22. Vigolo, B.; Penicaud, A.; Coulon, C.; Sauder, C.; Pailler, R.; Journet, C.; Bernier, P.; Poulin, P. Macroscopic Fibers and Ribbons of Oriented Carbon Nanotubes. *Science* **2000**, *290*, 1331–1334.
23. Erison, L. M.; Fan, H.; Peng, H.; Davis, V. A.; Zhou, W.; Sulpizio, J.; Wang, Y.; Booker, R.; Vavro, J.; Guthy, C.; et al. Macroscopic, Neat, Single-Walled Carbon Nanotube Fibers. *Science* **2004**, *305*, 1447–1450.
24. Jiang, K.; Li, Q.; Fan, S. Spinning Continuous Carbon Nanotube Yarns. *Nature* **2002**, *419*, 801.
25. Zhang, M.; Aktinson, K. R.; Baughman, R. H. Multifunctional Carbon Nanotube Yarns by Downsizing an Ancient Technology. *Science* **2004**, *306*, 1358–1361.
26. Zhang, X.; Jiang, K.; Feng, C.; Liu, P.; Zhang, L.; Kong, J.; Zhang, T.; Li, Q.; Fan, S. Spinning and Processing Continuous Yarns from 4-Inch Wafer Scale Super-Aligned Carbon Nanotube Arrays. *Adv. Mater.* **2006**, *18*, 1505–1510.
27. Yun, Y. H.; Shanov, V.; Tu, Y.; Subramaniam, S.; Schulz, M. J. Growth Mechanism of Long Aligned Multiwall Carbon Nanotube Arrays by Water-Assisted Chemical Vapor Deposition. *J. Phys. Chem. B* **2006**, *110*, 23920–23925.
28. Pint, C. L.; Xu, Y. Q.; Pasquali, M.; Hauge, R. H. Formation of Highly Dense Aligned Ribbons and Transparent Films of Single-Walled Carbon Nanotubes Directly from Carpets. *ACS Nano* **2008**, *2*, 1871–1878.
29. Cao, A.; Xu, C.; Liang, J.; Wu, D.; Wei, B. X-ray Diffraction Characterization on the Alignment Degree of Carbon Nanotubes. *Chem. Phys. Lett.* **2001**, *344*, 13–17.
30. Zhang, H.; Cao, G. P.; Wang, Z.; Yang, Y.; Shi, Z.; Gu, Z. Influence of Hydrogen Pretreatment Condition on the Morphology of Fe/Al_2O_3 Catalyst Film and Growth of Millimeter-Long Carbon Nanotube Array. *J. Phys. Chem. C* **2008**, *112*, 4524–4530.
31. Cao, A.; Dickrell, P. L.; Sawyer, W. G.; Ghasemi-Nejhed, M. N.; Ajayan, P. M. Super-Compressible Foamlike Carbon Nanotube Films. *Science* **2005**, *310*, 1307–1310.